

# Operando Analysis of Electron Accumulation in Titanium(IV) Oxide Particles in an Aqueous Suspension Using a Photoacoustic Spectroscopic Method

著者	Murakami Naoya, Shinoda Tatsuki
journal or publication title	The Journal of Physical Chemistry C
volume	123
number	1
page range	222-226
year	2018-12-13
URL	<a href="http://hdl.handle.net/10228/00007713">http://hdl.handle.net/10228/00007713</a>

doi: info:doi/10.1021/acs.jpcc.8b10566

# Operando Analysis of Electron Accumulation in Titanium(IV) Oxide Particles in an Aqueous Suspension Using a Photoacoustic Spectroscopic Method

*Naoya Murakami,<sup>1,2,\*</sup> Tatsuki Shinoda<sup>2</sup>*

<sup>1</sup>Department of Applied Chemistry, Faculty of Engineering, Kyushu Institute of Technology, 1-1 Sensuicho, Tobata, Kitakyushu 804-8550, Japan

<sup>2</sup>Graduate School of Life Science and Systems Engineering, Kyushu Institute of Technology, 2-4 Hibikino, Wakamatsu-ku, Kitakyushu 808-0196, Japan

## ABSTRACT

The time course of photoabsorption of an aqueous suspension of titanium(IV) oxide (TiO<sub>2</sub>) particles was studied using photoacoustic (PA) spectroscopy. In the absence of an electron acceptor and the presence of an electron donor, ultraviolet (UV) irradiation increased PA intensity because photoabsorption of the suspension increased due to trivalent titanium (Ti<sup>3+</sup>) species generated by electron accumulation in TiO<sub>2</sub> particles. In contrast, the addition of methylene blue (MB) as an acceptor caused a decrease in PA intensity, indicating that accumulated electrons were

consumed by reduction of MB to colorless leuco-MB. The results for various TiO<sub>2</sub> particles indicated that Ti<sup>3+</sup> density is determined by this method. Moreover, the measurement can be applicable to quantitative operando analysis for accumulated electrons in a photocatalytic reaction.

## INTRODUCTION

Titanium(IV) oxide (TiO<sub>2</sub>) is a representative semiconductor photocatalyst that is used as a photofunctional material for environmental remediation.<sup>1,2</sup> A photocatalytic reaction using bandgap excitation is induced by excited electrons and positive holes. Both of these species are often assumed to be consumed simultaneously by a redox reaction or recombination. However, excited electrons and positive holes are not always consumed at the same time if excited electrons or positive holes are stabilized in a certain state and accumulated in the semiconductor. Some metal oxide semiconductors, including TiO<sub>2</sub>, tungsten(VI) oxide (WO<sub>3</sub>) and molybdenum(VI) oxide, are known to have electron accumulation properties. Electron accumulation is induced by electron trapping at a metal ion with an oxygen vacancy in the semiconductor. For example, a possible structure of electron accumulation in TiO<sub>2</sub> is thought to be trivalent titanium (Ti<sup>3+</sup>) species, and it is considered that defective sites can be empirically measured by evaluation of Ti<sup>3+</sup>.<sup>3</sup> In the absence of electron acceptors, the accumulated electrons continue to be stabilized unless positive holes are generated. On the other hand, in the presence of electron acceptors electrons that have accumulated on the surfaces of particles can react with the acceptors if the accumulated electrons are trapped in a shallow energy level that is more negative than the redox potential of the acceptor. Thus, only reduction proceeds in the dark while oxidation reaction by positive holes does not take place. Such a photocatalytic reaction has been studied as a reductive energy storage system using

TiO<sub>2</sub>-WO<sub>3</sub><sup>4-7</sup> and as hydrogenation of carbonyl compounds by accumulated electrons<sup>8-11</sup>. However, there has been no quantitative analysis of electrons that accumulated on semiconductor particles during the photocatalytic reaction, though reduced products have been analyzed in most studies.

For a TiO<sub>2</sub> sample, accumulated electrons, i.e., Ti<sup>3+</sup> are known to show photoabsorption in the visible to near-infrared region. Therefore, absorption spectroscopy enables operando analysis of Ti<sup>3+</sup> under a photocatalytic condition. We carried out quantitative analysis of photogenerated Ti<sup>3+</sup> in TiO<sub>2</sub> particles under gas phase using photoacoustic spectroscopy (PAS).<sup>12-15</sup> PAS is one type of absorption spectroscopy that is applicable to even opaque and strongly scattering materials because it detects photoabsorption indirectly through photothermal waves generated by relaxation of the photoexcited states.<sup>16,17</sup> However, observation of Ti<sup>3+</sup> in a photocatalytic suspension reaction has not been achieved using PAS because volatile components from the suspension can negatively affect the microphone as a detector of PAS. Recently, we have developed a PAS system for photoabsorption of a suspension using a corrosion-resistant photoacoustic (PA) cell, which enables evaluation of a suspension under various conditions.<sup>18</sup>

In the present study, we studied the time course of accumulation of electrons in an aqueous suspension of TiO<sub>2</sub>. Accumulation of electrons was observed by changes in PA intensity attributed to Ti<sup>3+</sup> species. Moreover, we showed that the PA method used in the present study is applicable to operando analysis of accumulated electrons in a photocatalytic reaction.

## **EXPERIMENTAL**

## Materials

Ten kinds of TiO<sub>2</sub> powder samples from commercial sources, ST-21, ST-41, CR-EL (Ishihara Sangyo Co.), AMT-100, AMT-600, MT-150A (TAYCA Co.), super-titania F6A, super-titania G1 (Showa Denko Co.), commercial brookite (Kojundo Chemical Laboratory Co.) and reference catalyst JRC-TIO-1 supplied by the Catalysis Society of Japan were used. The crystal structures of ST-21, ST-41, AMT-100, AMT-600, super-titania F6A, and JRC-TIO-1 are mainly anatase, while those of MT-150A, CR-EL, super-titania G1 are mainly rutile powders. Analytical-grade reagents including methylene blue (MB), ethanol, and other chemicals were used without further purification. Aqueous suspensions were prepared by adding 200 mg of TiO<sub>2</sub> to 10 mL of aqueous ethanol solution (50 vol %). The suspensions were then treated by ultrasound for 30 min. Then 1.5 mL of the suspension was transferred into the cuvette of the PA cell and air was purged off from the cuvette by passing argon through the suspension for 15 min.

## PAS measurements

Detailed setups for PAS measurements were reported previously.<sup>18</sup> A homemade PA cell with an acrylic body and a quartz window was used. For measurements in a suspension sample, the PA cell was attached to a UV-transparent disposable cuvette with a 6 mm $\phi$  hole, which was covered with a cover glass (Matsunami glass, 0.04-0.06 mm). The setup is shown in Fig. 1. A laser diode emitting light at 532 nm (Edmund Optics, 84-930, 15 mW) was used as the probe light for detection of Ti<sup>3+</sup> species, and its output intensity was modulated by a function generator (NF, DF1906) at 2.6 Hz. As with the aforementioned experiments, the illumination pathway to the sample was through the window on top of the PA cell, and the illumination continued during measurements.

In addition to the illumination, the sample was illuminated with ultraviolet (UV) irradiation for excitation of TiO<sub>2</sub> through the cuvette, which was on the opposite side of the probe light, using a light-emitting diode (Nichia NCSU033B, emitting around 365 nm, 8.7 mW cm<sup>-2</sup>). During measurements, the headspace of the cuvette was purged using argon and the suspension was magnetically stirred.

The digital PA signal was acquired by a digital MEMS microphone (STMicroelectronics Inc., STEVAL-MKI155V2) buried in the cell and recorded using a PC equipped with a digital I/O interface. Time-series data were acquired by analog conversion of the digital PA signal followed by Fourier transform with a Hamming window function. The time-course data were obtained at ca. 20-s intervals.

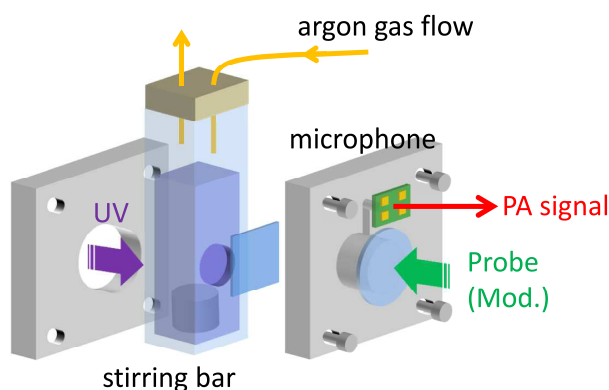


**Figure 1.** Schematic illustration of the PA cell.

## RESULTS AND DISCUSSION

### Increase in PA intensity due to electron accumulation in a time-course curve

Figure 2a shows time-course curves of PA intensity of the aqueous TiO<sub>2</sub> suspension containing ethanol under an argon atmosphere. Before UV irradiation, a trace of PA intensity attributed to background photoabsorption by the inner wall of the cell was observed, and its intensity was constant regardless of time. This is reasonable because the color of the suspension used in the experiments was white, and color change did not occur without UV irradiation. After UV irradiation, PA intensity increased and approached saturation with longer irradiation. Actually, the color of the suspension changed from white to gray-blue. The most probable candidate for the color change is Ti<sup>3+</sup> generated by electron accumulation as a counterpart of hole consumption by ethanol. A similar result was obtained in previous PAS measurement of TiO<sub>2</sub> powders in a gaseous atmosphere containing argon and methanol vapor.<sup>13</sup> However, the time taken for reaching a saturation limit in the present study was longer despite high intensity of UV light than that in the previous study (saturation time of over 15 min, UV light intensity of 2.8 mW cm<sup>-2</sup>)<sup>13</sup>. One possibility is due to difference of electron donor. Another possibility is that a larger amount of TiO<sub>2</sub> particles was irradiated by UV light with stirring, and the number of producible Ti<sup>3+</sup> species in the present study was larger than that in the previous study<sup>13</sup>.

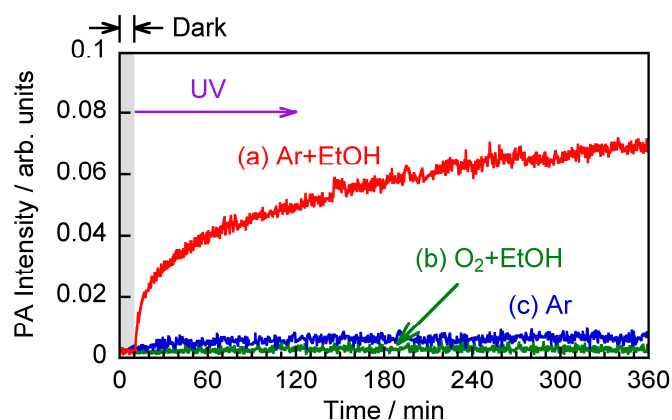


**Figure 2.** Time-course curves of PA intensity of aqueous TiO<sub>2</sub> (brookite) suspensions (a) containing ethanol under an argon atmosphere, (b) containing ethanol under an oxygen atmosphere, and (c) with no ethanol under an argon atmosphere.

In order to confirm that the increase in PA intensity is due to Ti<sup>3+</sup>, a control experiment was carried out. In the presence of oxygen, saturated PA intensity was much smaller than that measured in the absence of oxygen (Fig. 2b). This is presumably due to retardation of Ti<sup>3+</sup> generation by oxygen, which works as an electron acceptor. Such saturation of PA intensity can be explained by the balance of generation and extinction of Ti<sup>3+</sup> by electron accumulation and oxidation by O<sub>2</sub>, respectively. A trace of PA intensity suggests that the extinction of Ti<sup>3+</sup> is faster than generation of Ti<sup>3+</sup>, and extinction of Ti<sup>3+</sup> is promoted due to efficient diffusion of O<sub>2</sub> by magnetic stirring. In the absence of ethanol (Fig. 2c), PA intensity was also small compared to that in the presence of the donor because hole consumption as a counterpart reaction of electron accumulation hardly occurs in the absence of ethanol. A trace of PA intensity is presumably due to contaminated organic compounds on the surface of TiO<sub>2</sub>, which works as an electron donor.

### **Time-course curves of PA intensity of various TiO<sub>2</sub> samples**

In order to discuss the dependence of time-course curves on the kind of TiO<sub>2</sub>, various TiO<sub>2</sub> samples were measured. Figure 3 shows time-course curves of representative TiO<sub>2</sub> samples. All of the samples showed similar curves, though their saturation limits and rate constants of increase in PA intensity were different. Saturation tendency of PA intensity suggests that the number of

sites giving  $\text{Ti}^{3+}$  is limited depending on the kind of  $\text{TiO}_2$  sample. Therefore, saturated PA intensity was estimated from the time-course curves to discuss  $\text{Ti}^{3+}$  density. Figure 4 shows the relationship between saturated PA intensity and  $\text{Ti}^{3+}$  density determined in previous studies<sup>13,15</sup>. The relationship seems to show a positive correlation, but saturated PA intensity was not proportional to  $\text{Ti}^{3+}$  density. This is probably because not only  $\text{Ti}^{3+}$  density but also optical properties have an influence on PA intensity. Therefore, another experiment is required to estimate  $\text{Ti}^{3+}$  density from the time-course curve of PA intensity.

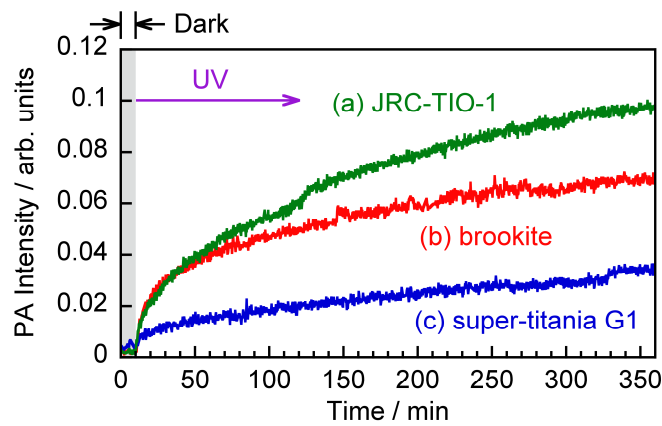


**Figure 3.** Time-course curves of PA intensity of (a) JRC-TIO-1, (b) brookite, and (c) super-titania G1 suspensions containing (a) ethanol under an argon atmosphere.

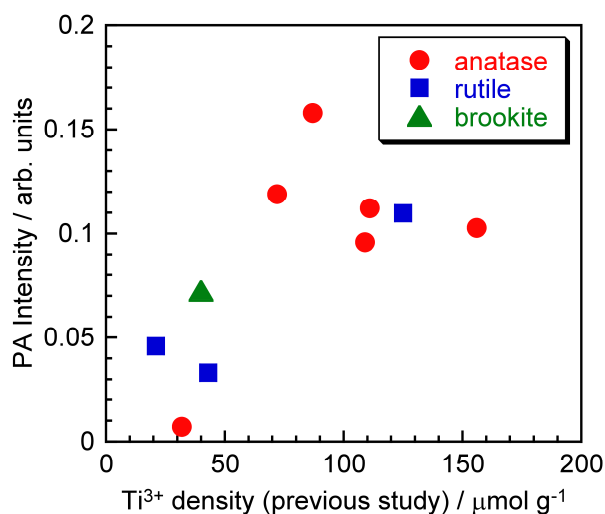


**Figure 4.** Relationship between saturated PA intensity and Ti<sup>3+</sup> density reported in ref. 13 and ref. 15.

#### Decrease in PA intensity due to electron transfer in a time-course curve

Figure 5 shows time-course curves of PA intensity of an aqueous TiO<sub>2</sub> suspension containing ethanol under an argon atmosphere after UV turn-off. The PA intensity was constant after UV turn-off because there are no acceptors that can be reduced by accumulated electrons in the suspension. Thus, accumulated electrons are stabilized permanently unless an electron acceptor is added to the suspension. In contrast, PA intensity rapidly decreased after addition of MB, and the blue color due to MB also disappeared. It is well known that leuco-methylene blue (LMB), which is a colorless product with an absorption peak at 256 nm, is generated in the absence of oxygen via reduction through the following mechanism.<sup>19,20</sup>



Since  $\text{TiO}_2$  has a conduction band with a more negative potential than that for reduction of MB to LMB, some of the accumulated electrons possibly reduce MB to LMB. Therefore, the decay in PA intensity is attributed to the consumption of  $\text{Ti}^{3+}$  through electron transfer from  $\text{Ti}^{3+}$  to MB. Actually, the gray-blue color of the suspension faded when MB was added. Some studies have shown that surface  $\text{Ti}^{3+}$  behaves as a reaction site as well as an adsorption site via electron donation and that its efficiency depends on the energy levels of accumulated electrons.<sup>21-28</sup> Therefore, the approach of PA intensity to the initial value by addition of MB as shown in Fig. 5 may indicate that accumulated electrons in a shallow energy level react with electron acceptors. In contrast, some sample showed PA intensity around the equivalence point, which is much different from the initial value. This indicates that accumulated electrons are stabilized in the bulk and/or deep energy level. Such a difference is possibly reasonable because the energy levels of  $\text{Ti}^{3+}$  depends on kind of the sample<sup>15</sup> though adsorption properties of MB on  $\text{Ti}^{3+}$  site may have an influence on such a difference.

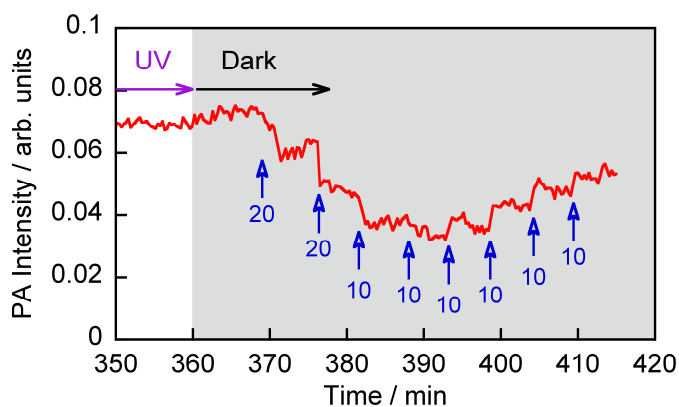


**Figure 5.** Time-course curve of PA intensity of an aqueous  $\text{TiO}_2$  (brookite) suspension containing ethanol under an argon atmosphere after UV turn-off. The arrows denote addition of MB ( $10 \text{ mmol L}^{-1}$ ), and numbers under the arrows are amounts of MB.

The addition of more than the equivalence point of MB conversely increased PA intensity, while a blue color attributed to MB was observed in the suspension. This indicates that an excess amount of MB was maintained in the suspension without being reduced to LMB. Thus, PA intensity at this time is attributed to absorption of not  $Ti^{3+}$  but MB around 532 nm.

### Estimation of $Ti^{3+}$ density

Figure 6 shows PA intensity of the suspension after addition of MB as a function of MB amount. This relationship can be used as not only a calibration curve for obtaining the amount of accumulated electrons from PA intensity but also the equivalence point for determination of  $Ti^{3+}$  density. From data around the equivalence point in this figure, the equivalence point can be estimated using the following equations,

$$I(v) = \begin{cases} -s_1(v - v_{EP}) + I_{EP} & (v < v_{EP}) \\ s_2(v - v_{EP}) + I_{EP} & (v \geq v_{EP}) \end{cases} \quad (2)$$

where  $s_1$  and  $s_2$  are the slope,  $v$  ( $\mu\text{L}$ ) is the amount of MB added,  $v_{EP}$  ( $\mu\text{L}$ ) is the equivalence point,  $I$  is PA intensity after addition of  $v$  of MB, and  $I_{EP}$  is PA intensity at the equivalence point. With consideration of two-electron reduction for MB to leuco-MB as shown in eq. 1,  $Ti^{3+}$  density can be calculated from the  $v_{EP}$  value as follows,

$$D = 2 \cdot v_{EP} \cdot M/w \quad (3)$$

where  $D$  ( $\text{mol g}^{-1}$ ) is  $Ti^{3+}$  density,  $M$  ( $\text{mol L}^{-1}$ ) is the concentration of MB, and  $w$  (g) is the weight of  $TiO_2$  included in the suspension. Ratio of the  $v_{EP}$  value obtained using  $20 \text{ g L}^{-1}$  of  $TiO_2$  (Fig.

6a) to that obtained using  $10 \text{ g L}^{-1}$  of  $\text{TiO}_2$  (Fig. 6b) was about 2.4 though it should be 2 according to Eq. 3. This is presumably attributed to experimental error for the  $\nu_{\text{EP}}$  value obtained using  $10 \text{ g L}^{-1}$  of  $\text{TiO}_2$  due to small PA intensity.

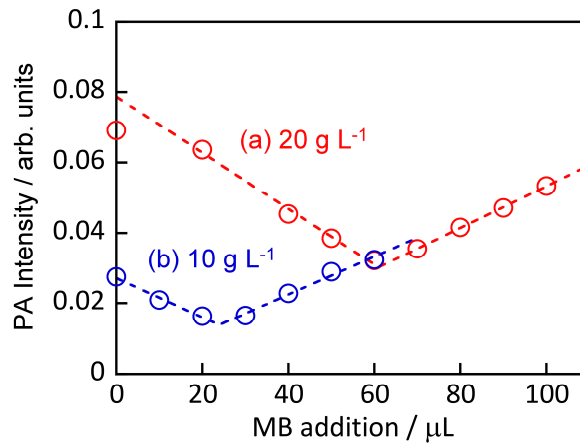


**Figure 6.** PA intensity of the suspension containing (a)  $20 \text{ g L}^{-1}$  and (b)  $10 \text{ g L}^{-1}$  of  $\text{TiO}_2$  after addition of MB as a function of MB amount.

Figure 7 shows the relationship of  $D$  with  $\text{Ti}^{3+}$  density obtained by the photochemical method, which uses the surface reaction of  $\text{Ti}^{3+}$  with methyl viologen to generate its cation radical, in previous studies<sup>13,15</sup>. The  $D$  values are nearly proportional to  $\text{Ti}^{3+}$  density obtained in both studies, suggesting that assignment of the PA signal to  $\text{Ti}^{3+}$  is reasonable. Slope of extrapolation line in Fig. 7 was about 0.7. This indicates that the  $D$  values estimated from the present study is smaller than that of previous study. Plausible reason for it is that stronger electron donor, i.e., methanol and triethanolamine were used as hole scavenger in the previous study.

The PAS technique used in the present study has advantages over the photochemical method<sup>3</sup>: (A1) the time required for estimation is shorter than that for estimation by the photochemical

method, which needs more than 1 day, and (A2) the time course of  $\text{Ti}^{3+}$  accumulation can be monitored. In comparison to PAS measurement in gas phase<sup>13</sup>, (B1) calibration using standard  $\text{TiO}_2$  powder of which the  $\text{Ti}^{3+}$  density has already been quantified is not needed because  $\text{Ti}^{3+}$  density can be directly calculated from the equivalence point, and (B2) pH control of the suspension and utilization of various acceptors is possible.

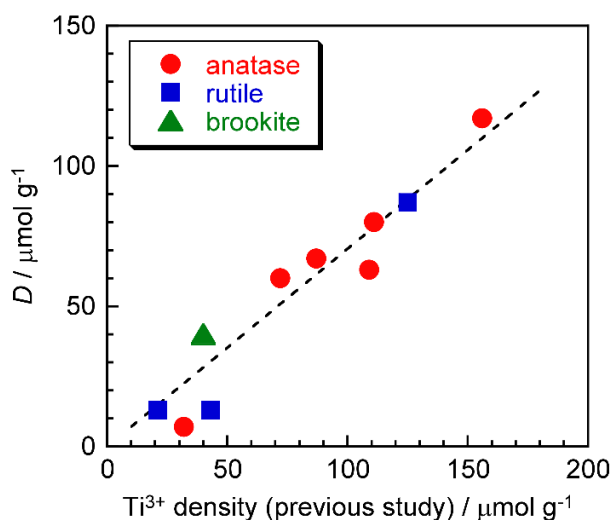


**Figure 7.** Relationship of  $D$  with the  $\text{Ti}^{3+}$  density reported in ref. 13 and ref. 15.

## CONCLUSION

We have proposed a method for operando analysis of electron accumulation and transfer under a photocatalytic suspension condition using the PA technique. This method enables further analysis of the kinetics of accumulation of electrons on  $\text{TiO}_2$  particles included in the suspension by changing pH and acceptors with various redox potentials. Moreover, the PA technique is an alternative method for easy and precise estimation of  $\text{Ti}^{3+}$  density on  $\text{TiO}_2$  powders. Therefore,

we believe that this method has a potential for operando analysis of photocatalytic particles including TiO<sub>2</sub> and other semiconductor particles.

## AUTHOR INFORMATION

### Corresponding Author

Naoya Murakami (murakami@life.kyutech.ac.jp)

## ACKNOWLEDGMENT

This work was supported by Grant-in-Aid for Scientific Research(C) (Grant Number 17K06019) and Grant-in-Aid for Scientific Research on Innovative Areas “Innovations for Light-Energy Conversion (I<sup>4</sup>LEC)” (Grant Number 18H05172).

## REFERENCES

- (1) Hoffmann, M. R.; Martin, S. T.; Choi, W.; Bahnemann, D. W. Environmental Applications of Semiconductor Photocatalysis. *Chem. Rev.* **1995**, *95*, 69–96.
- (2) Fujishima, A.; Rao, T. N.; Tryk, D. A. Titanium Dioxide Photocatalysis. *J. Photochem. Photobiol. C: Photochem. Reviews* **2000**, *1*, 1–21.
- (3) Ikeda, S.; Sugiyam, N.; Murakami, S.; Kominami, H.; Kera, Y.; Noguchi, H.; Uosaki, K.; Torimoto, T.; Ohtani, B. Quantitative Analysis of Defective Sites in Titanium(IV) Oxide Photocatalyst Powders. *Phys. Chem. Chem. Phys.* **2003**, *5*, 778–783.

- (4) Tatsuma, T.; Saitoh, S.; Ohko, Y.; Fujishima, A. TiO<sub>2</sub>-WO<sub>3</sub> Photoelectrochemical Anticorrosion System with an Energy Storage Ability. *Chem. Mater.* **2001**, *13*, 2838–2842.
- (5) Tatsuma, T.; Saitoh, S.; Ngaotrakanwiat, P.; Ohko, Y.; Fujishima, A. Energy Storage of TiO<sub>2</sub>-WO<sub>3</sub> Photocatalysis Systems in the Gas Phase. *Langmuir* **2002**, *18*, 7777–7779.
- (6) Ngaotrakanwiat, P.; Tatsuma, T.; Saitoh, S.; Ohko, Y.; Fujishima, A. Charge–discharge Behavior of TiO<sub>2</sub>–WO<sub>3</sub> Photocatalysis Systems with Energy Storage Ability. *Phys. Chem. Chem. Phys.* **2003**, *5*, 3234–3237.
- (7) Ngaotrakanwiat, P.; Tatsuma, T. Optimization of Energy Storage TiO<sub>2</sub>–WO<sub>3</sub> Photocatalysts and Further Modification with Phosphotungstic Acid. *J. Electroanal. Chem.* **2004**, *573*, 263–269.
- (8) Kohtani, S.; Yoshioka, E.; Saito, K.; Kudo, A.; Miyabe, H. Adsorptive and Kinetic Properties on Photocatalytic Hydrogenation of Aromatic Ketones upon UV Irradiated Polycrystalline Titanium Dioxide: Differences between Acetophenone and Its Trifluoromethylated Derivative, *J. Phys. Chem. C* **2012**, *116*, 17705–17713.
- (9) Kohtani, S.; Kamoi, Y.; Yoshioka, E.; Miyabe, H. Kinetic Study on Photocatalytic Hydrogenation of Acetophenone Derivatives on Titanium Dioxide. *Catal. Sci. Technol.* **2014**, *4*, 1084–1091.
- (10) Kohtani, S.; Kurokawa, T.; Yoshioka, E.; Miyabe, H. Photoreductive Transformation of Fluorinated Acetophenone Derivatives on Titanium Dioxide: Defluorination vs. Reduction of Carbonyl Group. *Appl. Catal. A: Gen.* **2016**, *521*, 68–74.

- (11) Kohtani, S.; Kawashima, A.; Miyabe, H. Reactivity of Trapped and Accumulated Electrons in Titanium Dioxide Photocatalysis. *Catalysts* **2017**, *7*, 303.
- (12) Murakami, N.; Mahaney, O.O.P.; Torimoto, T.; Ohtani, B. Photoacoustic Spectroscopic Analysis of Photoinduced Change in Absorption of Titanium(IV) Oxide Photocatalyst Powders: A Novel Feasible Technique for Measurement of Defect Density. *Chem. Phys. Lett.* **2006**, *426*, 204–208.
- (13) Murakami, N.; Mahaney, O.O.P.; Abe, R.; Torimoto, T.; Ohtani, B. Double-Beam Photoacoustic Spectroscopic Studies on Transient Absorption of Titanium(IV) Oxide Photocatalyst Powders. *J. Phys. Chem. C* **2007**, *111*, 11927–11935.
- (14) Maeda, K.; Murakami, N.; Ohno, T. Dependence of Activity of Rutile Titanium(IV) Oxide Powder for Photocatalytic Overall Water Splitting on Structural Properties. *J. Phys. Chem. C* **2014**, *118*, 9093–9100.
- (15) Murakami, N.; Shinoda, T. Mid-infrared Absorption of Trapped Electrons in Titanium(IV) Oxide Particles Using a Photoacoustic FTIR Technique. *Phys. Chem. Chem. Phys.* **2018**, *20*, 24519–24522.
- (16) Rosencwaig, A.; Gersho, A. Theory of the Photoacoustic Effect with Solids. *J. Appl. Phys.* **1976**, *47*, 64–69.
- (17) Tam, A.C. Applications of Photoacoustic Sensing Techniques. *Rev. Mod. Phys.* **1986**, *58*, 381–431.

- (18) Murakami, N.; Maruno, H. In Situ Photoacoustic Spectroscopic Analysis on Photocatalytic Decolorization of Methylene Blue over Titanium(IV) Oxide Particles. *RSC Adv.*, **2016**, *6*, 65518–65523.
- (19) Mills, A. An Overview of the Methylene Blue ISO Test for Assessing the Activities of Photocatalytic Films. *Appl. Catal. B: Environ.* **2012**, *128*, 144–149.
- (20) Impert, O.; Katafias, A.; Kita, P.; Mills, A.; Pietkiewicz-Graczyk, A.; Wrzeszcz, G. Kinetics and Mechanism of a Fast Leuco-methylene Blue Oxidation by Copper(II)–halide Species in Acidic Aqueous Media. *Dalton Trans.* **2003**, 348–353.
- (21) Lu, G.; Linsebigler, A.; Yates Jr., J. T.  $\text{Ti}^{3+}$  Defect Sites on  $\text{TiO}_2(110)$ : Production and Chemical Detection of Active Sites. *J. Phys. Chem.* **1994**, *98*, 11733–11738.
- (22) Rodriguez, J. A.; Jirsak, T.; Liu, G.; Hrbek, J.; Dvorak, J.; Maiti, A. Chemistry of  $\text{NO}_2$  on Oxide Surfaces: Formation of  $\text{NO}_3$  on  $\text{TiO}_2(110)$  and  $\text{NO}_2 \leftrightarrow \text{O}$  Vacancy Interactions. *J. Am. Chem. Soc.* **2001**, *123*, 9597–9605.
- (23) Shiraishi, Y.; Togawa, Y.; Tsukamoto, D.; Tanaka, S.; Hirai, T. Highly Efficient and Selective Hydrogenation of Nitroaromatics on Photoactivated Rutile Titanium Dioxide. *ACS Catal.* **2012**, *2*, 2475–2481.
- (24) Shiraishi, Y.; Hirakawa, H.; Togawa, Y.; Sugano, Y.; Ichikawa, S.; Hirai, T. Rutile Crystallites Isolated from Degussa (Evonik) P25  $\text{TiO}_2$ : Highly Efficient Photocatalyst for Chemoselective Hydrogenation of Nitroaromatics. *ACS Catal.* **2013**, *3*, 2318–2326.

- (25) Shiraishi, Y.; Hirakawa, H.; Togawa, Y.; Hirai, T. Noble-Metal-Free Deoxygenation of Epoxides: Titanium Dioxide as a Photocatalytically Regenerable Electron-Transfer Catalyst. *ACS Catal.* **2014**, *4*, 1642–1649.
- (26) Hirakawa, H.; Katayama, M.; Shiraishi, Y.; Sakamoto, H.; Wang, K.; Ohtani, B.; Ichikawa, S.; Tanaka, S.; Hirai, T. One-Pot Synthesis of Imines from Nitroaromatics and Alcohols by Tandem Photocatalytic and Catalytic Reactions on Degussa (Evonik) P25 Titanium Dioxide. *ACS Appl. Mater. Interfaces* **2015**, *7*, 3797–3806.
- (27) Hirakawa, H.; Hashimoto, M.; Shiraishi, Y.; Hirai, T. Selective Nitrate-to-Ammonia Transformation on Surface Defects of Titanium Dioxide Photocatalysts. *ACS Catal.* **2017**, *7*, 3713–3720.
- (28) Hirakawa, H.; Hashimoto, M.; Shiraishi, Y.; Hirai, T. Photocatalytic Conversion of Nitrogen to Ammonia with Water on Surface Oxygen Vacancies of Titanium Dioxide. *J. Am. Chem. Soc.* **2017**, *139*, 10929–10936.